

Cite this: *Energy Environ. Sci.*,
2022, 15, 1156

Reline deep eutectic solvent as a green electrolyte for electrochemical energy storage applications†

Sara Azmi,  Masoud Foroutan Koudahi and Elzbieta Frackowiak *

Deep eutectic solvents (DESs) are an environmentally benign promising emerging class of versatile solvent systems. In this paper, for the first time, a new approach to the DES application of choline chloride–urea, commonly called Reline, and its aqueous mixtures as eco-friendly, affordable and anticorrosive electrolytes for carbon-based electrochemical capacitors (ECs) is proposed. The symmetric ECs operating in the Reline-based electrolyte demonstrate excellent electrochemical stability at a voltage of 2.2 V, in turn supplying a high energy. Furthermore, by adding 1 wt% water to the DES system, the specific capacitance increased from 100 to 157 F g⁻¹ at a 1 A g⁻¹ current load. In addition, excellent long-term capacitor stability was achieved up to >25 000 cycles for the Reline + 1% water-electrolyte and >50 000 cycles for pure Reline. The paramount benefit is the fact that Reline-based ECs are constructed in ambient conditions as opposed to ECs operating with organic electrolytes and ionic liquids (ILs) demanding glove-box. Additionally, the Reline-based electrolyte is a non-flammable solution. Moreover, the current collectors of our DES-based supercapacitor do not corrode. Therefore, the present findings have important implications to extend the application of the green, non-toxic and cheap Reline DES electrolyte for high-performance ECs with a wide voltage window and a superior lifespan.

Received 17th September 2021,
Accepted 13th January 2022

DOI: 10.1039/d1ee02920g

rsc.li/ees

Broader context

Following an eco-friendly strategy, the choline–urea deep eutectic solvent, named Reline, is a promising non-flammable green electrolyte, just like ILs, but is low-cost, biodegradable and non-toxic. Its tuneable properties and anti-corrosion characteristics make the application of Reline suitable in several fields, particularly in electrochemical capacitors (ECs). The performance of ECs is directly linked to the cell operating voltage, which is limited for an aqueous electrolyte-based EC (1.23 V). Moreover, an extension of the maximum voltage causes accelerated ageing and corrosion of electrode materials and current collectors. Nevertheless, the use of Reline as an EC electrolyte offers an advantageous and cost-effective solution having, in addition to its anticorrosive character, a stable electrochemical window. Our report enlightens the electrochemical performance of carbon-based supercapacitors based on pure Reline and its water mixture as electrolytes. It has been proven that pure Reline and slightly hydrated Reline offer excellent cycle stability at 2.2 V with superb capacitance retention. The current research provides new insights into the development of a reliable, environmentally friendly electrolyte to produce highly durable ECs (50 000 cycles). It can be useful for many applications, especially smart technologies for e-skin wearable electronics as well as hybrid electric vehicles, and military and space industries, alone or integrated with other energy storage devices.

Introduction

Energy storage is a major strategic worldwide issue. Reducing the production of greenhouse gases requires the use of renewable sources of energy. Due to the intermittency of some of these sources, particularly photovoltaics, storage is the only solution that can be used to offset the time between electricity production

(by solar panels operating only during the day) and the satisfaction of demand (lighting at night). Nowadays, the most widely used system to store energy for all applications is undoubtedly electrochemical storage.¹ Among various energy storage systems, an electrochemical capacitor (EC) is an efficient device used when a high power density is required.² It has a much higher capacitance than the traditional dielectric capacitors sold in markets and a much lower energy density but a higher power capacity than batteries.³ Therefore, electrochemical capacitors have the characteristics of being a practical bargain between traditional capacitors and batteries.⁴ Principally, ECs comprise three constituents: electrodes that are commonly carbon-based materials, an electrolyte that could be aqueous or non-aqueous and a

Institute of Chemistry and Technical Electrochemistry, Poznan University of Technology, Berdychowo 4, Poznan 60-965, Poland.

E-mail: elzbieta.frackowiak@put.poznan.pl

† Electronic supplementary information (ESI) available. See DOI: 10.1039/d1ee02920g



separator.⁵ There is a vast selection of electrode materials and electrolytes used for designing ECs. However, there is growing interest in carbon-based capacitors since these materials are accessible, low-cost and possess various morphologies with high stability and conductivity.⁶ The charge storage mechanism of ECs is based on electrostatic interactions at the electrode/electrolyte interfaces through an electrical double layer formed at the positively and negatively charged electrodes.⁷ Over time, extensive literature has described different carbonaceous materials used as active electrodes for ECs, which included graphene,⁸ carbon nanotubes,⁹ activated carbon¹⁰ and carbon fibers.¹¹ Most early studies and the current work focus on the use of the graphene carbon material due to its specific surface area (SSA) of 2630 m² g⁻¹ theoretically, high electrical conductivity, mechanical flexibility and high capacitive performance (theoretically ≈ 550 F g⁻¹).¹² Indeed, the three-dimensional (3D) macroscopic graphene material has been proposed by several researchers as a great technological promise for supercapacitors providing good performance due to its high porosity offering fast ionic diffusion.^{13,14} However, activated carbon, including Black Pearl (BP2000) and YP80F, displays high tuneable properties with a wide surface area, making it the most suitable porous material for electrochemical capacitors.¹⁵

So far, more studies have been focused on the electrode materials of supercapacitors,^{6,15} while being less involved in the field of electrolytes. The choice of a suitable electrolyte for electrochemical capacitors remains one of the most challenging problems. The electrolytes of ECs could be divided into three classes: aqueous (KOH, LiNO₃, *etc.*), organic (based on acetonitrile, ethylene carbonate, *etc.*), and ionic liquids (BMI-PF₆, EMI-TFSI, *etc.*).⁵ At the same time, new types of electrolytes named deep eutectic solvents (DESs) start to be investigated aiming to increase the operating voltage of the EC devices, thanks to their excellent electrochemical stability.

DESs are green solvents formed by quaternary ammonium salts with hydrogen donors in a specific ratio forming eutectics.¹⁶ These solvents have similar properties to ionic liquids (ILs), namely, a wide liquid range, water compatibility, low vapour pressure and non-volatility,¹⁷ but are the most promising environmentally benign and cost-effective alternatives.¹⁸ The first DES system reported, which was investigated by Abbott in 2003, contained the quaternary ammonium salt choline chloride (ChCl) and urea in a molar ratio of 1:2.¹⁹ Both choline chloride and urea are biodegradable, non-toxic, and readily available components. More recently attention has been focused on deep eutectic solvents (DESs) as new green solvents which have been applied in the fields of electrochemistry,^{20–22} materials growth,²³ catalysis,²⁴ biotransformation,²⁵ extraction and separation,²⁶ gas and liquid adsorption^{27,28} and corrosion resistance²⁹ due to their low cost, biodegradability and low toxicity. Although several applications of DESs have been investigated, little interest has been placed on DESs as electrolytes for electrochemical energy storage technologies.

DESs share many characteristics with ILs³⁰ but their low cost makes them particularly attractive in many applications, including electrolytes for energy devices. Due to their unique

properties, despite their extremely high cost, ILs found a wide range of applications in various electrochemical devices including lithium-ion batteries,^{31–33} fuel cells,³⁴ dye-sensitized solar cells,³⁵ *etc.* Like ILs, DESs were also used in electrochemistry as electrolytes for supercapacitors (SCs) due to their wider electrochemical stability window, which increases the energy density of SCs.

The appearance of DESs in the field of SCs may present an attractive option for electrolytes. Li *et al.* used a DES-based supramolecular gel polymer electrolyte in EDLCs which delivered an operating voltage of 2.4 V.³⁶ Vorobiov *et al.* adopted a chitosan-supported DES as a bio-based electrolyte for flexible supercapacitors with a 1.6 V operating window.³⁷ Zhong *et al.* reported a study using a choline chloride–ethylene glycol-based DES as an electrolyte for wide temperature range supercapacitors with an operating voltage of 2 V.³⁸ In the same context, Sathyamoorthi and co-workers investigated also the use of a non-fluoro DES for high-temperature supercapacitors with a 1.3 V maximum cell voltage.¹⁷ Furthermore, Zaidi *et al.* employed a DES based on *N*-methylacetamide and lithium salt as the electrolyte at high temperatures for activated carbon-based supercapacitors with an operating window of 1.8 V.³⁹ A most recent study⁴⁰ highlights the design of a wide voltage window (2.4 V) DES using tetraethylammonium bromide (TEAB) and ethylene glycol for electrochemical capacitor applications. Recently, Amara *et al.* proposed the application of the lithium bis(fluorosulfonyl)imide and *N*-methylacetamide DES as a superionic electrolyte for activated carbon electrochemical double-layer capacitors.⁴¹ Karade reported the use of a DES as an electrodeposition synthesis bath for hybrid supercapacitor electrodes operating in aqueous electrolytes.⁴² It is worth noting that there are only a few detailed reports on the application of DESs in the field of electrochemical capacitors (ECs).

As far as we know, no previous research has mentioned the use of the choline–urea deep eutectic solvent (DES) as an electrolyte for energy storage systems, especially electrochemical capacitors (ECs). Indeed, the choline–urea DES, also known commercially as Reline, is a biodegradable, non-toxic and inexpensive eutectic mixture of choline chloride and urea in a 1:2 molar ratio. It is obtained from low-cost and environmentally friendly starting materials.⁴³ Moreover, choline chloride is known to be an important nutrient that performs essential metabolic functions necessary for the formation of vital bodily substances needed for animal nutrition.⁴⁴ Besides, urea is a versatile organic substance with a high nutrient density and good handling and storage properties present in different industries, mostly cosmetics⁴⁵ (anti-ageing and dry skincare) and agriculture^{46,47} (fertilizers).

A choline–urea eutectic mixture has highly appropriate physical properties which make it useful as a solvent in the field of electrochemistry, especially for electrochemical capacitors, since it has a large stable electrochemical window of about 3–4 V and high chemical and thermal stability.⁴⁸ Furthermore, being a green corrosion inhibitor, Reline is widely considered to be a good candidate to prevent corrosion of metals and alloys.^{29,49,50} It has been used for corrosion protection of less noble metals,²³ especially copper and stainless steel.⁴⁹ Ibrahim



et al. investigated the effective corrosion inhibitors of Reline DES and its water mixture for copper, mild steel and stainless steel 316.⁴⁹ Their study confirms the effectiveness of Reline DES as a corrosion inhibitor in a harsh acidic environment even with a moisture content up to 10 wt%.⁴⁹ This characteristic is an asset for its application as an electrolyte for electrochemical capacitors considering the need for protection of the current collector during long lifetime cycling. The intriguing aspect in the field of electrochemical capacitors is the condition under which the device is assembled and operated, mainly the Reline DES preparation is easy, cost-effective and does not involve any post-purification or glovebox use.⁵¹ However, most of the DESs including Reline suffer from their high viscosity which influences directly their conductivity.⁵²

To counter the aforementioned drawback in the case of Reline which is a water-soluble electrolyte,⁴⁹ it has been investigated and reported that a small fraction of water can remarkably improve the electrolyte system by significantly reducing its viscosity and relatively increasing its ionic conductivity.^{52,53} Several studies have been conducted to point out the thermo-physical properties^{50,52,54–57} and dynamics^{43,58} of pure Reline and its mixture. As mentioned by Sapir *et al.*, water is usually added to improve the physicochemical properties of DESs, notably Reline.⁵⁴ In this context, we tried to explore and benefit from Reline (DES) and its mixture with water at different proportions as an attractive electrolyte for supercapacitors.

Following an eco-friendly strategy, this work reports, for the first time, the investigation of the choline-urea DES as an electrolyte for carbon-based electrochemical capacitors (ECs). Its anti-corrosion properties and high electrochemical stability play an important multifunctional role in energy storage.

Experimental section

Materials

Graphite powder (particle diameter $\leq 20 \mu\text{m}$, 95–99.99% purity) was supplied by Graphit Kropfmühl GmbH, Germany. Black Pearl 2000 (BP2000) and YP80F powders were provided by Cabot[®], USA and Kuraray, Japan, respectively. Other chemicals, including H_2SO_4 (ACS reagent, 95.0–98.0%), NaNO_3 (ACS

reagent, $\geq 99.0\%$), KMnO_4 (ACS reagent, $\geq 99.0\%$), H_2O_2 (30 wt% in H_2O , ACS reagent), choline chloride ($\geq 98\%$), and urea (ACS reagent, ≥ 99 – 100%) were purchased from Sigma-Aldrich[®] (Poland).

Reline deep eutectic solvent preparation

Reline deep eutectic solvent was prepared from choline chloride ($\text{C}_5\text{H}_{14}\text{ClNO}$) salt in combination with urea ($\text{CH}_4\text{N}_2\text{O}$) hydrogen bond donors (HBDs) by adjusting the 1:2 molar ratio (Fig. 1a). The mixture was heated at $80 \text{ }^\circ\text{C}$ with continuous stirring until a homogeneous colourless liquid was formed. Additionally, further Reline-water mixtures were prepared by adding desired quantities of distilled water to Reline DES at different percentages (0.05%, 1%, 2%, and 5%). No additional purification was done for all experiments. The resulting DES solutions were used as electrolytes for supercapacitors. The electrical conductivity, density and dynamic viscosity of the pure choline-urea deep eutectic solvent and its water mixtures were investigated using a conductivity meter (Mettler Toledo[®], Switzerland) and a Lovis 2000 M/ME micro-viscometer (Anton Paar), respectively. The accuracy associated with density measurements is $\leq 0.0001 \text{ g cm}^{-3}$. The conductivity of pure DES was studied for the temperature range from $25 \text{ }^\circ\text{C}$ to $160 \text{ }^\circ\text{C}$ through the use of electrochemical impedance spectroscopy. The residual water content of Reline DES was measured using a Karl-Fisher coulometer. The absorption spectra of the Reline DES and its water mixtures were recorded utilizing a PerkinElmer FTIR spectrophotometer with a resolution of 4 cm^{-1} . The thermal properties of the DES were investigated using a NETZSCH DSC 204F1 Phoenix differential scanning calorimeter (DSC). Initially, the calibration was done under a N_2 -atmosphere through liquid-nitrogen cooling. A few drops of Reline DES were sealed in an aluminium crucible; the samples were first cooled from room temperature up to $-120 \text{ }^\circ\text{C}$, then heated up to $50 \text{ }^\circ\text{C}$ at a rate of $1 \text{ }^\circ\text{C min}^{-1}$.

3DG hydrogel electrode preparation

Graphene oxide (GO) was synthesized following modified Hummers' method, reported elsewhere,⁵⁹ and subsequently was used for the preparation of the three-dimensional graphene like material (3DG) using the hydrothermal self-

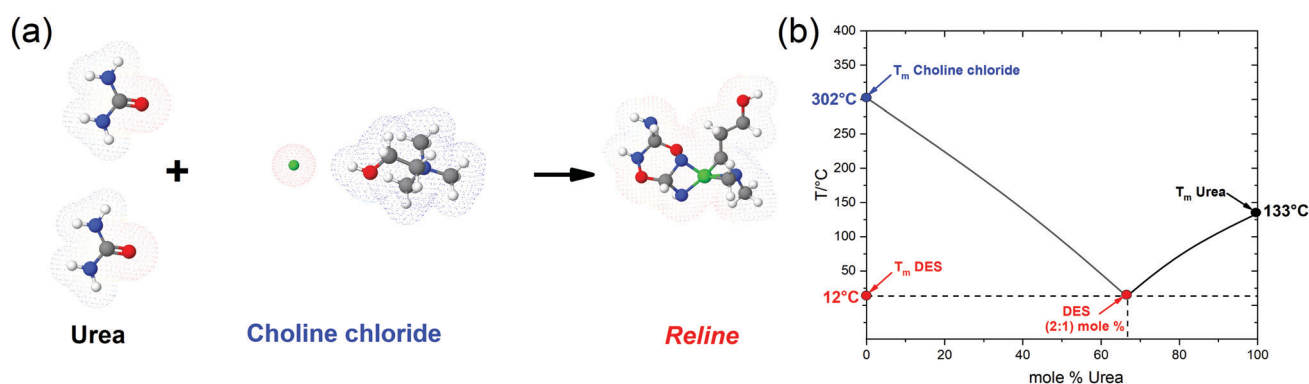


Fig. 1 (a) Molecular representation and synthesis of Reline DES; ●: Cl, ○: H, ●: O; ●: C; ●: N. (b) Solid-liquid equilibrium phase diagram of the choline chloride-urea mixture (Reline DES).



assembly process. Briefly, GO with a proper concentration was sonicated in DI water for 2 h using an ultrasonic bath (temperature ≤ 25 °C). Afterwards, the dispersed sample was poured into a Teflon-lined stainless steel autoclave and maintained at 200 °C for 12 h without any disturbance. Later, the resulting 3DG was soaked in DI water for one week to remove the residual impurities. For physical characterization, 3DG was lyophilized to an aerogel for 72 h using a freeze-drying setup. The resulting electrode was characterized by Brunauer–Emmett–Teller (BET) isothermal analysis (77 K) with N_2 as the adsorbate (ASAP 2460, Micromeritics, USA) to evaluate the surface area and porosity of the samples. Further morphology investigation was done using scanning electron microscopy (SEM) analysis.

The preparation of electrode materials based on 3DG was carried out without the addition of any binder or additive, and by cutting self-standing, disk-shaped pellets with a diameter of 8 mm and a thickness of ~ 1 mm. Before assembling the cells, the electrodes based on 3DG were pressed to a thickness of ~ 200 μm . Electrode materials based on powdered BP2000 and YP80F were prepared as follows: 90% of BP2000 and YP80F, 5 wt% of the poly(tetrafluoroethylene) (PTFE) binder (60% suspension in water) and 5% of C65 conductive carbon black were mixed using isopropanol as the solvent. The constituents were combined in a mortar to ensure the homogeneity of the ingredients in the obtained thick slurry. Later, the resulting pastes were pressed and rolled with a thickness of 150 to 200 μm using a calendaring machine. Finally, electrodes with a diameter of 10 mm were cut and dried in a dryer at 60 °C for 24 h.

Electrochemical characterization

For this purpose, the prepared electrodes, as well as the separator, were soaked in the electrolyte for 24 h to allow complete infiltration of highly viscous electrolyte molecules into the pores. The used separator was a glass microfiber membrane (GF/A, Whatman™) with a thickness of 260 μm and a disc diameter of 12 mm. A Swagelok cell with stainless steel current collectors was used for assembling symmetrical cells based on carbon electrodes. Three electrode cells equipped with a reference electrode were used to monitor the behaviour of single electrodes separately. The electrochemical behaviour of the samples was studied using a multi-channel potentiostat/galvanostat (VMP3, Biologic, France). Cyclic voltammetry (CV) at sweep rates from 5 mV s^{-1} to 200 mV s^{-1} , galvanostatic charge–discharge (GCD) at 0.5, 1, and 2 A g^{-1} current densities, and electrochemical impedance spectroscopy in the frequency range from 100 kHz to 1 MHz (at 0 V) were conducted.

Results and discussion

Choline chloride–urea (Reline) DES phase diagram

Generally, DES is formed by the combination of two constituents generating a new liquid phase characterized by a lower freezing point compared to that of individual products. The molecular structure of Reline components is presented in Fig. 1(a), whereas

Fig. 1(b) shows the phase diagram of the choline chloride–urea mixture as a function of the molar composition. As presented in the figure, choline chloride and urea have melting points (T_m) of 302 and 133 °C, respectively. The DES mixture possesses the lowest melting point of 12 °C. Thus, the choline chloride–urea eutectic mixture is formed at a composition of 67 mol% urea which means that two urea molecules are required to complex the chloride anions of choline for obtaining the eutectic mixture.

Thermophysical properties of Reline DES

The Reline DES might contain some water traces depending on the raw material pre-treatment. In this study, the DES preparation was done without any purification/drying of the used chemicals. The residual water content of the prepared Reline was found to be 1900 ppm using the Karl-Fischer coulometry method. It is well known that the conductivity and viscosity have important effects on the properties of Reline deep eutectic solvent.⁵ The experimentally determined viscosities, densities and conductivities of Reline and its mixture with water content are shown in Table 1. The viscosity and density data of pure Reline DES were retrieved from the literature.⁵³ The reported data cover the defined range of water percentages from 0.05% to 5% at 25 °C. From the presented table, it is clear that increasing the water quantity leads to an increase in conductivity. As reported in the literature,⁶⁰ the high viscosity of the DES is in virtue of the broad hydrogen bond network present between each component which leads to a lower mobility of free species within the DES. Indeed, by adding water to the DES solution, it reacts with the H bond donor which is urea in the case of Reline that makes the hydrogen bond network less extensive and creates more flexible mobility. Thus, the conductivity will be increased by the increase of water content.⁵⁴

The ionic conductivity of choline–urea electrolytes is a critical parameter for the performance of a supercapacitor because it is responsible for the ion mobility and the number of charge carriers of the system.⁶¹ Table S1 (ESI†) presents the temperature dependence of the Reline DES over the temperature range of 25–150 °C. As it can be noticed from the figure, the DES conductivity varies from 1.5 mS cm^{-1} at 25 °C to 180 mS cm^{-1} at 150 °C. This is due to the decrease of the DES viscosity as the temperature increases. The observed temperature dependences of conductivity are well fitted by the Arrhenius equation (eqn 1):

$$\sigma = \sigma_0 \exp\left(\frac{-E_a}{K_b T}\right) \quad (1)$$

Table 1 Density ($\rho/\text{g cm}^{-3}$), viscosity ($\eta/\text{mPa s}^{-1}$) and electrical conductivity (mS cm^{-1}) of Reline in various water mixtures at pressure $p = 0.1$ MPa and $T = 25$ °C

	Density ($\rho/\text{g cm}^{-3}$)	Viscosity ($\eta/\text{mPa s}^{-1}$)	Electrical conductivity (mS cm^{-1})
Pure DES	1.199 ^a	1750 ^a	1.3
0.5% water	1.172	172.9	4.11
1% water	1.170	76.32	7.06
2% water	1.168	31.11	11.72
5% water	1.159	13.39	16.76

^a Literature data.⁵³



where σ_0 is the conductivity of the pre-exponential factor, E_a is the activation energy, K_b is the Boltzmann constant, and T is the absolute temperature.

The Arrhenius plot of the temperature dependence of conductivity for the Reline DES is depicted in Fig. 2(a). The activation energy calculated from the slope of the plot and the Arrhenius equation is $21.17 \text{ kJ mol}^{-1}$ which is relatively comparable to the values reported for dried and water-saturated ILs.⁶² This indicates that the Reline DES ions require low energy for migration in highly conducting samples.

In order to assess the ionicity of DES electrolytes, the Walden classification diagram is an effective tool to compare the ionicity of the Reline DES-based system to other ILs and DESs. This plot illustrates the relationship between the conductivity and viscosity according to the Walden rule, $\Lambda\eta^2 = k$, where Λ is the molar conductivity ($\text{S cm}^2 \text{ mol}^{-1}$), η is the viscosity (Pa s^{-1}), and k is the constant estimated from the so-called ideal electrolyte solution KCl reference.⁶⁶ Fig. 2(b) depicts the Walden graph at room temperature for Reline DES and its water mixtures as well as other ILs taken from the literature. In detail, the solid blue line indicates the ideal Walden plot attributed to 1 M KCl solution and the deviation path and its magnitude from this line outlines the degree of ionization of the considered solutions. As illustrated in Fig. 2(b), the Walden plot distinguishes between the non-, poorly, good and super-ionic liquids. Pure Reline DES is classified as a poor ionic liquid at ambient temperature ($25 \text{ }^\circ\text{C}$) together with Ch:glycerine and LiNO_3 :NMAc DES systems. This is due to the hydrogen bonding in these DES systems leading to high viscosity and thus a limited conductivity. As expected, through the addition of water, the

Reline DES shifts from the poor ionic liquid class to a good ionic liquid offering better physical properties comparable to LiTFSI based ILs.

To outline the thermal properties of Reline DES, differential scanning calorimetry (DSC) measurements were carried out to characterize the exothermic, endothermic and glass transitions. Although the melting temperatures of choline chloride and urea are $\sim 302 \text{ }^\circ\text{C}$ and $\sim 133 \text{ }^\circ\text{C}$, respectively, the eutectic mixture temperature is lower ($\sim 12 \text{ }^\circ\text{C}$). The sample was initially cooled to $-120 \text{ }^\circ\text{C}$ (blue line) and then heated to $50 \text{ }^\circ\text{C}$ (green line), and the results are shown in Fig. 3(a). Upon heating the DES from $-120 \text{ }^\circ\text{C}$ to $60 \text{ }^\circ\text{C}$, the system displays a glass transition at $-53 \text{ }^\circ\text{C}$, followed by an exothermic cold crystallization peak at around $-20 \text{ }^\circ\text{C}$ and an endothermic melting peak starting at around $11 \text{ }^\circ\text{C}$ and ending at around $25 \text{ }^\circ\text{C}$. At temperatures ranging between 25 and $200 \text{ }^\circ\text{C}$, the DES is thermally stable. It was reported that this DES decomposes above $200 \text{ }^\circ\text{C}$ under two different stages related to choline chloride and urea partial decomposition.⁶⁹ Moreover, the properties of Reline DES and its water mixtures were investigated using infrared spectroscopy (IR) and the results are shown in Fig. 3(b). It can be noted that the characteristic spectrum of the Reline DES overlaps with those of its water mixtures (1%, 2% and 5%). This proves that the water addition does not change the structure of the Reline DES. For the IR spectrum of Reline, the dominant regions are the N-H and O-H stretching modes located between 3600 and 3000 cm^{-1} , and the NH_2 bending and C=O stretching bands detected between 1700 and 1600 cm^{-1} . Remarkably, the structure of the choline-urea mixture remains the same even after the addition of 5% of water, showing that the added water

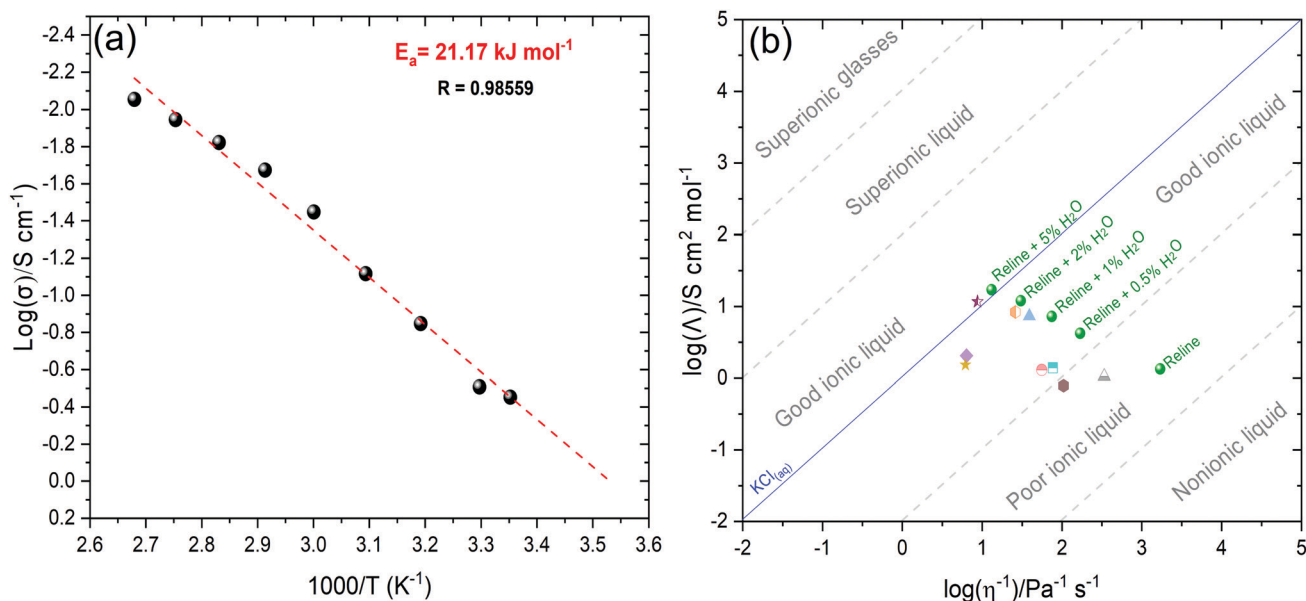


Fig. 2 (a) The Arrhenius plot concerning the ionic conductivity of the Reline DES electrolyte, (b) Walden plot at ambient temperature for: ● 1choline chloride (ChCl):2urea (Reline)^{this work}; ● ChCl:butanediol;⁶³ ▲ ChCl:ethylene glycol (EG);⁶³ ▲ ChCl:glycerine;⁶³ ◆ glutaronitrile (GLN):lithium bis(trifluoromethyl)sulfonyl]imide (LiTFSI);⁶⁴ ★ 2-methylglutaronitrile (MGLN):LiTFSI;⁶⁴ ■ LiTFSI:N-methylacetamide (NMAc);⁶⁵ ● (lithium nitrate) LiNO_3 :NMAc;³⁹ ★ lithium bis(fluorosulfonyl)-imide(LiFSI):formamide (FMD);⁴¹ ● tetraethylammonium chloride (TEAC):EG.⁴⁰ The blue line is the "ideal" Walden product line fixed with 1 mol L^{-1} aqueous KCl solution.



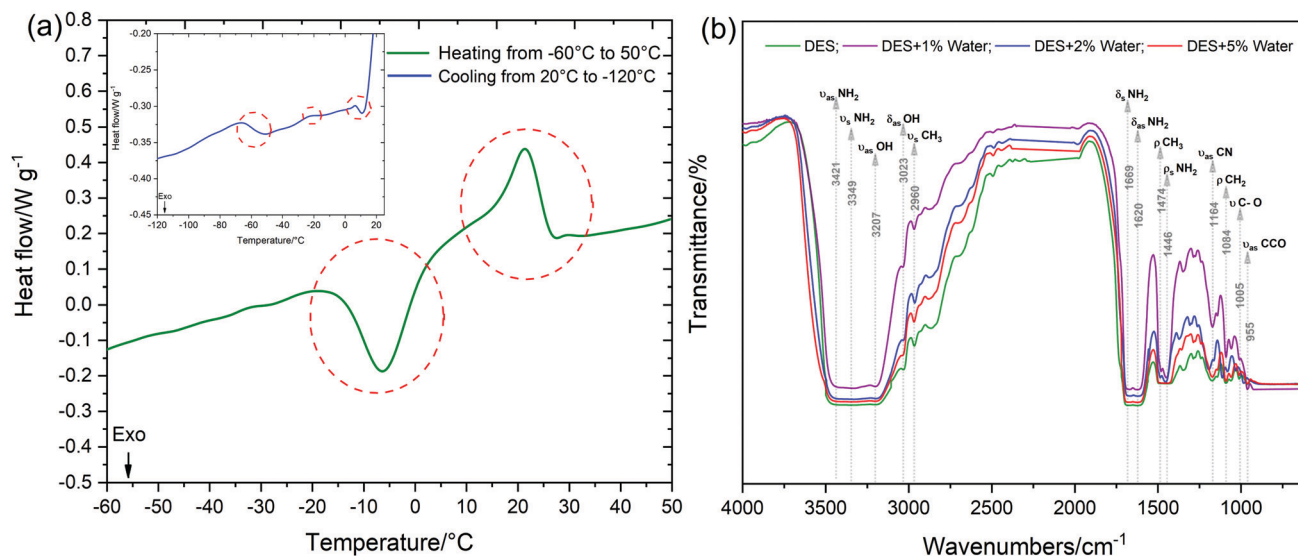


Fig. 3 (a) DSC thermogram of Reline DES; (b) FTIR spectrum of Reline DES and its water mixtures (1%, 2% and 5%).

has preferentially combined with the other water molecules present in the DES system.

Overall, the thermophysical properties of the Reline DES are dependent upon the temperature and the water content. Hence, the Reline DES as an electrolyte for supercapacitors could be improved by adding a low concentration of water in order to maintain the good ionic conductivity and consequently the high performance of the energy storage system.

Physicochemical characterization of carbon materials

In order to study the performance of the DES-based supercapacitors, the choice of an appropriate carbon electrode is inevitable. Thus, the principal factors that influence the supercapacitor electrode have been reported. Firstly, the specific surface area and the pore volume of the used carbon material have been studied using Brunauer-Emmett-Teller (BET) isothermal analysis (N₂ at 77 K). It can be seen from the isothermal curves in Fig. 4(a) that the three carbons present a small

hysteresis loop in the relatively high-pressure range that confirms the presence of the mesopores needed for good transport conditions across the electrode. The pore size distribution study of the three samples shows a dominance of the mesopore characters for 3DG and BP2000 carbons with pore volumes of 0.23 cm³ g⁻¹ and 1.9 cm³ g⁻¹, respectively, and a micropore texture for the YP80F material with a pore volume of 0.80 cm³ g⁻¹ (Fig. S1, ESI[†]). Further investigation of the electrode morphology was achieved using scanning electron microscopy. Fig. 4(b) depicts the SEM micrograph of the 3D graphene-like material synthesized by a hydrothermal process. A network of interconnected pores within a 3D structural material can be observed. It also reveals a relatively uniform distribution of large and small pores providing an accessible surface area. The 3DG macroporosity property will facilitate the transport process of ions and, therefore, improve the capacity and power density of the energy storage device, especially with the viscous character of the Reline DES electrolyte, while the

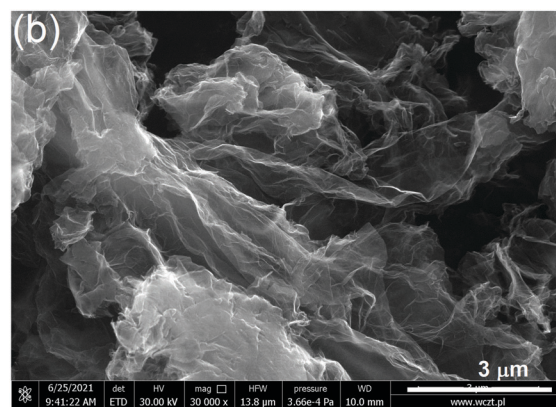
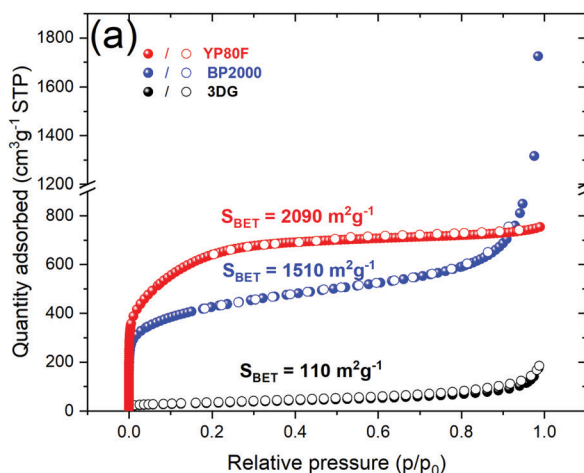


Fig. 4 (a) N₂ adsorption (●)/desorption (○) isotherms at 77K; (b) SEM image of the three-dimensional graphene-like material (3DG).



microtexture of the used activated carbon (BP2000 and YP80F) presents a significant difference compared to the 3DG material (Fig. S1 and S2, ESI†).

Electrochemical performance

To assess the application of pure DES and its water mixtures as electrolytes for supercapacitors, a symmetrical two-electrode system assembled using 3DG electrodes was subjected to electrochemical tests at room temperature. In the initial stage, the capacitive performance and the maximum operating voltage of the cells based on 3DG electrodes in DES, DES + 0.05% water, DES + 1% water, and DES + 5% water were evaluated by CV analysis and the results of the investigations are shown in Fig. 5(a–e). From the CV curves recorded at 5 mV s^{-1} , it can be seen that, with extending the voltage window from 1.5 V to 2.4 V, no obvious deviation from the initial, rectangular shape of CV (up to 1.5 V) was observed for 3DG in pure DES. However, the DES samples with water contents showed slight redox activities at the highest voltage, which can be taken as the sign of water decomposition. Therefore, the upper voltage stability limit was set at 2.2 V which is the start of the current response increase. From DES to DES + 1% water, the CV profiles exhibited a rectangular shape without deviation, which means that the charge storage is governed mainly by an electrostatic sorption/desorption process. Yet, with increasing the water content to 5%, an unstable CV profile including both capacitive and faradaic responses was obtained (Fig. 5(e)). This could be attributed to the electrolyte decomposition or the production of by-products/

surface groups that generate faradaic current during the sorption/desorption process.

Thus, it has further strengthened the conclusion reported by Du *et al.* regarding the non-stability of the electrochemical window of Reline DES when the water content is over 6%.⁵² Despite the drawbacks such as narrowing the operating voltage window or behaviour instability (for 5% H₂O content), the moderate presence of water molecules as additives (1%) enhances the conductivity, especially facilitating the transportation of ions inside porous electrodes. Therefore, the higher mobility of ions leads to a higher capacitance as well as a better power performance at higher scan rates. To evaluate the cell voltage limits, the galvanostatic charge/discharge (GCD) at 0.2 A g^{-1} was also applied for the pure DES electrolyte and its 1% water mixture with voltage extension from 1.5 to 2.2 V (Fig. 5(c and f)). It is clearly shown that, for both systems, the discharging area increases with the rise of the cell voltage. Interestingly, the GCD curves of the pure DES system reveal a relatively symmetrical triangular shape with a negligible decrease of the system energy efficiency which indicates the stability of the DES electrolyte at a higher voltage window and good matching of the DES ion size with the porous structure of 3DG, while the GCD curve of DES + 1% water displays a larger specific capacitance calculated from the discharge area but with a drop of the energy efficiency at a higher voltage. Table 2 presents the SC characteristics in various voltage ranges derived from galvanostatic discharge for 3DG (Fig. 5(c and d)) and BP2000 (Fig. S3(a and b), ESI†) electrodes. The formulas used to calculate the capacitive performance and efficiency at different voltages are summarized in the ESI.†

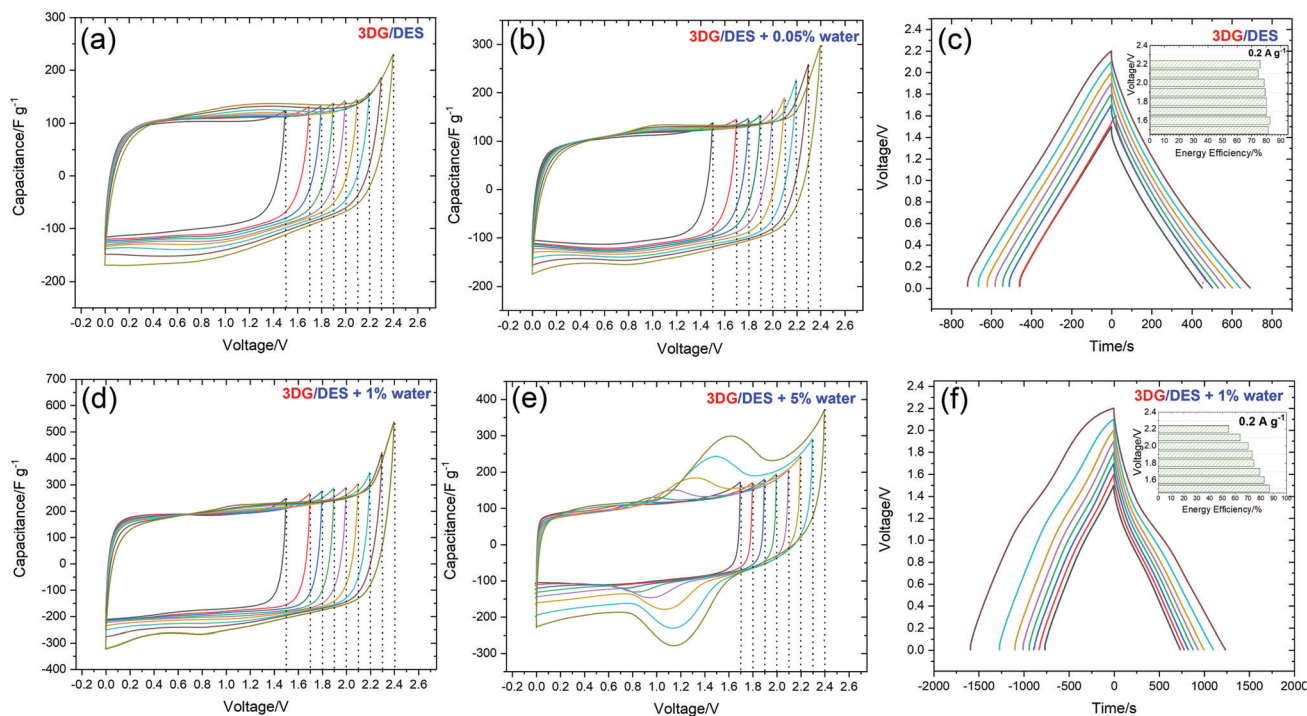


Fig. 5 CV curves at 5 mV s^{-1} of the 3DG electrochemical capacitor for (a) DES; (b) DES + 0.05% water (d) DES + 1% water and (e) DES + 5% water for various voltage extensions; GCD profiles of the cells at different voltage limits ranging from 1.5 to 2.2 V at 0.2 A g^{-1} using (c) the DES pure electrolyte and (f) DES + 1% water electrolyte.



For each voltage, the SC parameters were calculated based on the discharge time and by integrating the area under the galvanostatic discharge curve. By comparing the values reported in Table 2, it is noticed that the values calculated by integration are typically smaller than the ones estimated from discharge time. The capacitance (per one electrode) and specific energy of the system calculated by both methods show some differences. The extension of the voltage from 1.7 to 2.2 V leads to an increase of the capacitance of the four SCs. However, the energetic efficiency (η_E) displays a drop, especially at a higher voltage because of the deviation of the GCD curves from linearity at 0.2 A g⁻¹, especially for the 3DG SC in DES + 1% water (59%). The energy efficiency displays higher values when the GCD curves are recorded at 0.5, 1 and 2 A g⁻¹ (Fig. 9(c)). Further examinations of the SCs were performed using a two-electrode cell with an additionally positioned Hg/Hg₂SO₄ electrode and the result is shown in Fig. 6. These investigations show the linear trend of the GCD curves for the positive and negative electrodes at all the operating voltages. Interestingly, Reline DES electrolyte permits the voltage of the BP2000 based capacitor to be up to 1.7–2.2 V. At 2.2 V (Fig. 6(d)), the GCD discharge curve at the positive side shows a slight deviation in linearity which could have originated from the DES H-bond donor electroadsorption (urea).⁶⁷ Mamme *et al.* investigated the electrical double layer of the choline chloride–urea DES by molecular modelling.⁶⁷ They reported that the electroadsorption mechanism of urea on carbon electrodes depends on the intermolecular interactions and the surface polarization. They found that the electrode/electrolyte interface is composed of a flat arranged layer of urea, followed by a mixed charged cluster of all Reline components. Nevertheless, the electrostatic interaction of Reline DES is highly enhanced between urea and

the negatively charged electrode compared to the positively charged one. Moreover, in DES and its water mixture systems, the water preferentially combines with urea molecules but not with ChCl. Hence, the ChCl fraction linked with urea through hydrogen bonds will produce more free Ch⁺ leading to high ionic dissociation. As a result, the decomposition of water can be suppressed and the wide electrochemical window could be preserved. It can be confirmed that 2.2 V is the maximum safe voltage for SCs operating in Reline DES and Reline DES + 1% water. The high electrochemical stability window (ESW) of Reline was also evaluated from the investigation of the stability factor *S* originally proposed by Xu *et al.*⁶⁸ using (eqn (2)):

$$S = \frac{Q_{\text{charge}}}{Q_{\text{discharge}}} - 1; \quad (2)$$

Factor *S* is calculated from the cyclic voltammetry (CV) curve recorded in a three-electrode cell system obtained by progressively increasing the vertex potential range for each electrode.

According to equation (2), Q_{charge} and $Q_{\text{discharge}}$ present the charges stored and released during the positive and negative CV sweeps, respectively. The largest ESW for each electrode corresponds to $S < 0.1$. Before introducing the *S*-value analysis, it can be seen from the three-electrode cell investigations (Fig. S4(a), ESI[†]) that the performance of the full cell with separate behaviour of positive and negative electrodes displays a nearly rectangular square. The plot displayed in Fig. S4(b) (ESI[†]) predicts a stable potential window of about 2.2 V with $S < 0.1$ for the Reline DES SC device. Therefore, it was decided to perform all the other electrochemical investigations at 2.2 V. Fig. 7(a–d) summarizes the electrochemical performance of the ECs based on the pure DES electrolyte and its water mixtures recorded at different scan rates (5–200 mV s⁻¹) with a potential

Table 2 Comparison of SC parameters for 3DG (0.2 A g⁻¹) and BP2000 (0.5 A g⁻¹) based SCs operated in Reline DES and DES + 1% water

Electrode material	Electrolyte	U_{max} (V)	$C_{\text{el,GD}}$ (F g ⁻¹)	$C_{\text{el,int/GD}}$ (F g ⁻¹)	$E_{\text{s,GD}}$ (W h kg ⁻¹)	$E_{\text{s,int/GD}}$ (W h kg ⁻¹)	η_t (%)	η_E (%)		
3DG	Reline DES	1.7	110	105	19	11	100	81		
		1.8	104	97	18	11	100	81		
		1.9	105	94	18	12	99	80		
		2	106	96	18	13	98	79		
		2.1	107	93	18	14	98	79		
		2.2	111	96	19	16	97	78		
	Reline DES + 1% water	1.7	147	146	25	14	100	82		
		1.8	145	141	24	15	100	80		
		1.9	146	146	24	17	99	79		
		2	151	148	25	19	99	76		
		2.1	156	155	26	22	99	67		
		2.2	162	157	27	25	97	59		
		BP2000	Reline DES	1.7	74	65	16	9	100	82
				1.8	76	68	16	10	100	80
1.9	77			70	17	11	100	80		
2	78			68	17	12	100	76		
2.1	81			72	18	14	100	77		
2.2	84			76	18	16	99	75		
Reline DES + 1% water	1.7		80	71	17	8	100	83		
	1.8		82	72	18	9	99	80		
	1.9		84	74	18	10	98	78		
	2		87	78	19	11	97	79		
	2.1		90	79	19	12	98	77		
	2.2		92	85	20	14	97	78		



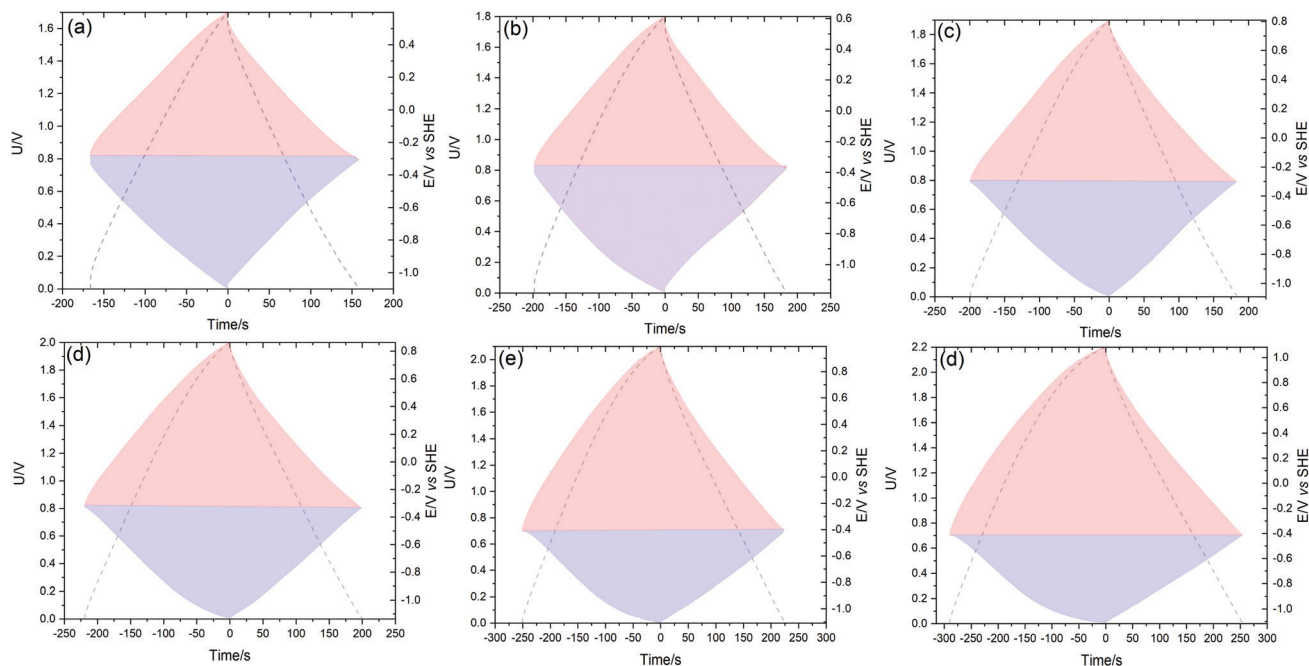


Fig. 6 GC/GD characteristics of two- and three-electrode cells using BP2000 electrodes in the Reline DES electrolyte at (a) $U_{\max} = 1.7$ V, (b) $U_{\max} = 1.8$ V, (c) $U_{\max} = 1.9$ V, (d) $U_{\max} = 2.0$ V, (e) $U_{\max} = 2.1$ V and (f) $U_{\max} = 2.2$ V.

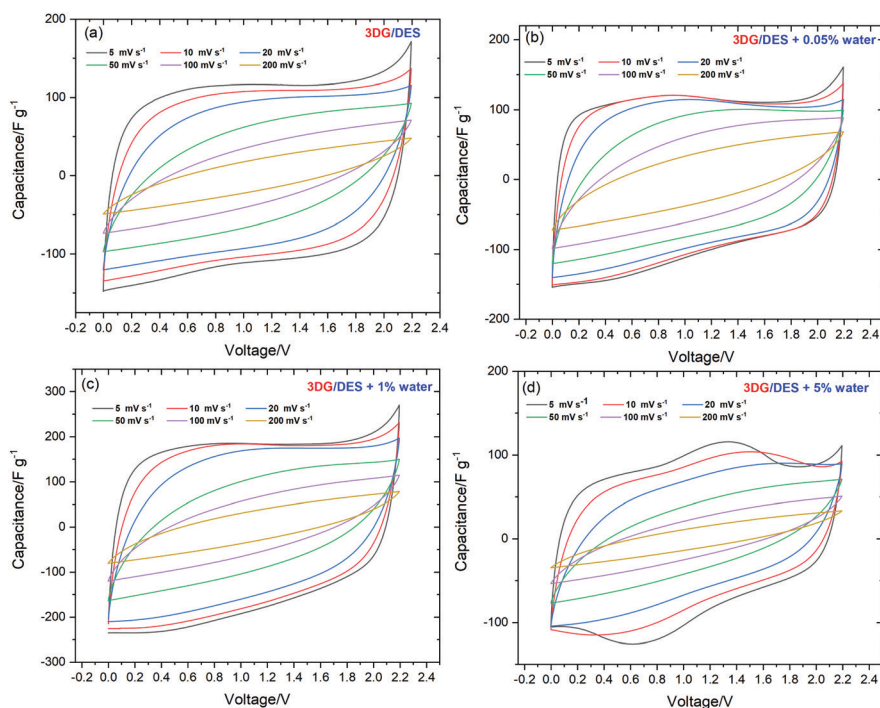


Fig. 7 CV curves at different scan rates under 2.2 V of (a) DES, (b) DES + 0.05% water, (c) DES + 1% water and (d) DES + 5% water.

window of 2.2 V. It can be noticed, at a low scan rate of 5 mV s^{-1} , the CV curves present a quasi-rectangular shape which demonstrates a good capacitive behaviour of the system.

Furthermore, it is highlighted that 3DG in the DES + 1% water system displays a high capacitance of 200 F g^{-1} at 5 mV s^{-1} . At the

same time, the 3DG in DES + 0.05% water showed a better power rate with maintaining its favourable capacitive performance in a wide range of sweep rates. To further evaluate the charge storage mechanism, electrochemical impedance spectroscopy measurements were carried out. Fig. 8 illustrates the Nyquist



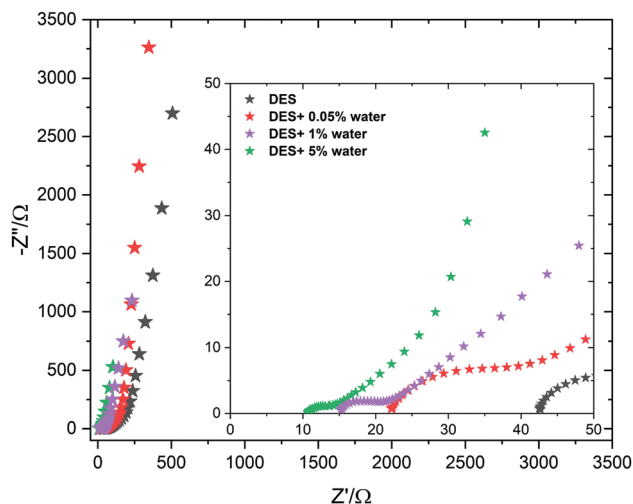


Fig. 8 Nyquist plots for the electrochemical capacitors operating in the DES and its water mixtures.

plots for 3DG electrodes in the ECs assembled using the pure DES and its mixtures with water at different percentages. The equivalent series resistance (ESR) for DES, DES + 0.05%, DES + 1%, and DES + 5% water can be estimated from the inset; the higher the amount of water, the lower the ESR value. The highest resistance was recorded for the pure DES electrolyte due to its high viscosity and low conductivity. Therefore, in the absence of water, 3DG in DES showed a wide semi-circle at high frequencies, indicating the existence of a considerable resistance against the

current flow at the interface of electrode/electrolyte. This is consistent with the obtained data from CV analysis: a higher ionic mobility leads to better transport properties. The galvanostatic charge–discharge curves recorded under different current densities (0.5 , 1 , and 2 A g^{-1}) of the DES electrolytes prepared with different water contents are compared in Fig. 9. Broadly speaking, a relatively symmetrical triangular shape of charge/discharge curves is noticed in all the samples at the three regimes with the specific capacitance increasing from 100 F g^{-1} to 157 F g^{-1} . However, the sample tested using DES + 5% water revealed a distortion from the ideal triangular shape which proves the presence of redox activity within the cells. The same distortions were observed in the CV profiles as well.

Interestingly, the GCD curves recorded from the pure DES and DES + 0.05% water have no visible differences in terms of specific capacitance, which demonstrates that, when adding small quantities of water ($<0.05\%$) to the Reline DES, no significant difference was observed in the electrochemical behaviour of the system. As expected, 3DG in DES + 1% water reached the highest specific capacitance per electrode (157 F g^{-1}) as well as the highest energy efficiency (70% at 0.5 A g^{-1}). It is clear that, when adding 1% of water to the pure DES electrolyte, the performance of the electrochemical cells at room temperature appears to be the best.

In the next stage, the long-term cyclic stability of 3DG in the pure DES and DES + 1% water was studied in order to highlight the long-term performance stability and the effect of adding water to the pure DES during continuous charge–discharge cycles.

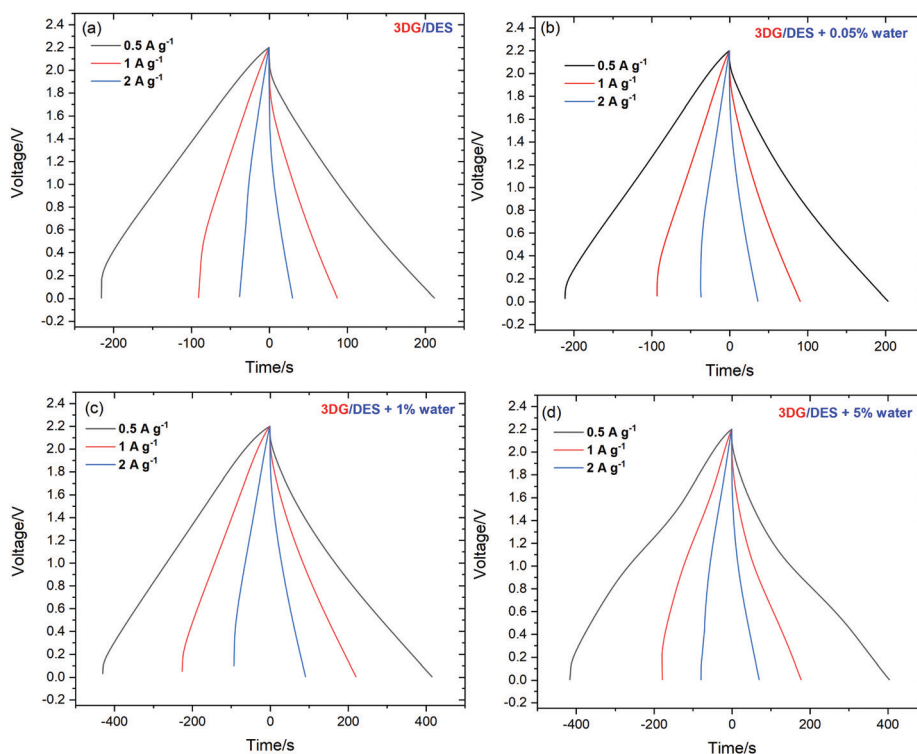


Fig. 9 GCD curves at 0.5 A g^{-1} , 1 A g^{-1} and 2 A g^{-1} of 3DG based ECs using (a) the pure Reline DES, (b) DES + 0.05% water, (c) DES + 1% water and (d) DES + 5% water.



Fig. 10(a and b) demonstrates the variation trend of specific capacitance *versus* cycle number. All samples showed a similar trend, including an initial sharp decrease, followed by stable behavior. After 25 000 repetitive charge–discharge cycles, 3DG in DES and DES + 1% water retained 90% and 88% of their initial capacitance values, respectively. These data reveal that the presence of at least 1% water does not have a tangible influence on the stability of electrolytes and the performance of ECs. The most striking result achieved from the data is the high stability of the 3DG capacitors using the pure Reline DES over 50 000 galvanostatic charge/discharge cycles at 1 A g^{-1} without an increase in the equivalent series resistance (ESR) value as presented in Fig. S5 (ESI[†]). This indicates the ability of the DES-based system to undergo superb stable charge–discharge cycles which highlights the anticorrosion properties of this electrolyte. The next important metric of the ECs is their ability to keep the charge. Electrochemical capacitors based on electrostatic attraction of ions usually show a high, spontaneous self-discharge in open-circuit voltage. It leads to a voltage drop and, subsequently, a decrease in operational energy density and power density.

In order to evaluate the self-discharge of 3DG in DES and DES + 1% water systems, the assembled cells were charged to specific voltage points (1.6, 1.8, 2.0 and 2.2 V) with a constant current load (1 A g^{-1}) and then kept at those voltages for 2 h before being left at an open-circuit voltage for 12 h. The next important metric of the ECs is their ability to keep the charge.

Electrochemical capacitors based on electrostatic attraction of ions usually show a high, spontaneous self-discharge in open-circuit voltage. It leads to a voltage drop and, subsequently, a decrease in operational energy density and power density. In order to evaluate the self-discharge of 3DG in DES and DES + 1% water systems, the assembled cells were charged to specific voltage points (1.6, 1.8, 2.0 and 2.2 V) with a constant current load (1 A g^{-1}) and then kept at those voltages for 2 h before being left at an open-circuit voltage for 12 h. Fig. 10(c and d) reveals the variation of cell voltage *versus* time. As can be seen from the figure, adding water to the pure DES causes a more rapid voltage drop, *i.e.*, quicker self-discharge which means that it reduces the system capability to maintain the applied voltage. Generally, each self-discharge plot can be divided into two or three parts depending on the system. Indeed, the two-stage plots are governed by a diffusion-controlled phenomenon, while the three-stage plots have diffusion-controlled and activation-controlled origins. It is apparent from Fig. 10c and d that the 3DG in the pure DES presents a two-diffusion-controlled-stage plot. The first stage represents a relatively sharp decrease as a result of charge redistribution, followed by a second step decrease which is caused by relocation of ions inside the pores.

By increasing the voltage from 1.6 to 2.2 V, no sign of a kinetically controlled phenomenon was noticed. With increasing the water content of the electrolyte, no binary-stage plot of voltage degradation was seen, rather the dominance of the activation controlled phenomenon resulted in the existence of

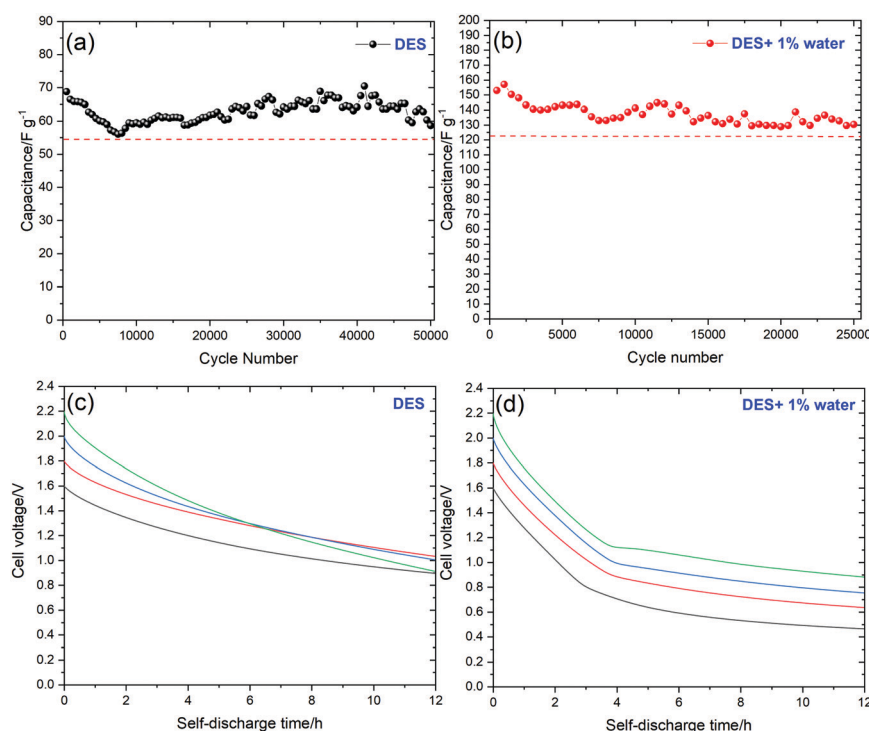


Fig. 10 (a) Long-term cycling (1 A g^{-1}) of the EC based on 3DG using the pure Reline DES at 2.2 V; (b) cycling performance of the EC based on 3DG (1 A g^{-1}) using DES + 1% water at 2.2 V; (c) the self-discharge over 12 h under open-circuit conditions of symmetric 3DG based capacitors using pure DES and (d) DES + 1% water electrolytes.



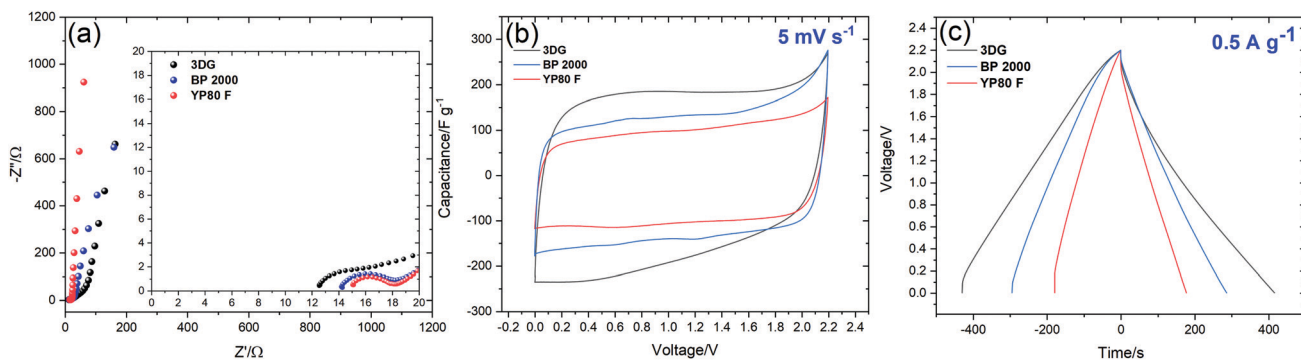


Fig. 11 Comparison of 3DG, BP2000 and YP80F based capacitors; (a) Nyquist plots; (b) CV curves at 5 mV s^{-1} ; (c) galvanostatic charge–discharge profiles tested at 0.5 A g^{-1} . Electrolyte: DES + 1% water.

three stages of sharp voltage decrease. As was expected, the presence of water in electrolytes decreases the overpotential of water decomposition, where, in the early stage, the diffusion-controlled process will be followed by an activation-controlled one. The Reline DES-based system displays the slowest self-discharge for all cut-off voltages. Such a phenomenon originates from its higher viscosity which reduces ion mobility and prevents ion relocation inside the pores.

Additionally, in order to extend the application of DES as an electrolyte for supercapacitors based on electrodes with different ion transport properties, two activated meso/microporous carbons (YP80F and BP2000) were electrochemically studied and compared to 3DG using DES + 1% water as an electrolyte, and the results are shown in Fig. 11. The Nyquist plots for 3DG, BP2000 and YP80F electrodes for supercapacitors assembled using DES + 1% water are depicted in Fig. 11(a). As illustrated, the equivalent series resistance (ESR) for the three ECs presents deviations related to the different porous nature of their electrodes. The Nyquist plot for the 3DG electrode-based EC presents the lowest ESR (12.5Ω) compared to BP2000 (14Ω) and YP80F (15Ω) ECs. Furthermore, the three ECs display a quasi-straight line in the low-frequency region, indicating the existence of typical capacitive behaviour.

However, the three insets indicate small semicircles at high frequencies probably related to the electrolyte viscosity. Fig. 11(b) depicts the CV curves of the three capacitors using DES + 1% water at 2.2 V recorded at 5 mV s^{-1} . At a lower scan rate, the CV curves of the three ECs present a rectangular shape leading to the conclusion that the charge storage system is governed by the electrostatic sorption/desorption process. However, some differences in the specific capacitance values, as well as a small deviation at the upper voltage limit (2.2 V), are visible. Thus, the 3DG based EC showed a higher capacitance, followed by BP2000 and YP80F. At a high scan rate, the BP2000 based system showed a better power rate with maintaining its favourable capacitive performance in a wide range of sweep rates (200 mV s^{-1}) (Fig. S7, ESI[†]). To outline the energy/power of the ECs based on the three carbon electrodes, galvanostatic charge–discharge measurements were performed at different current densities. Fig. 11(c) compares the charge–discharge profiles of 3DG, BP2000 and YP80F at 0.5 A g^{-1} . Generally, it

is apparent that the charge–discharge curves present nearly a good triangular shape. As shown in Fig. 11(c), the GCD curves of the supercapacitor based on the 3DG electrode at 2.2 V present the largest discharge area, followed by BP2000, while the YP80F system exhibits the smallest area. At the same time, the specific capacitances of 3DG, BP2000 and YP80F based on the integral area of discharge are 157 , 107 and 68 F g^{-1} , respectively. It seems that the three electrodes have displayed a good electrochemical performance with a 70% energy efficiency for the 3DG sample, 72% for BP2000 and 57% for YP80F. This comparison led us to confirm the wide application of the Reline DES as a very promising electrolyte for carbon-based supercapacitors. Additionally, energy density and power density are the most important parameters for evaluating supercapacitor performance. Fig. 12 illustrates the power density and energy density by Ragone plots of the 3DG electrode-based supercapacitors using DES and DES + 1% water. Another EC was tested using Li_2SO_4 electrolyte in order to highlight the difference between aqueous and deep eutectic solvent-based supercapacitors.

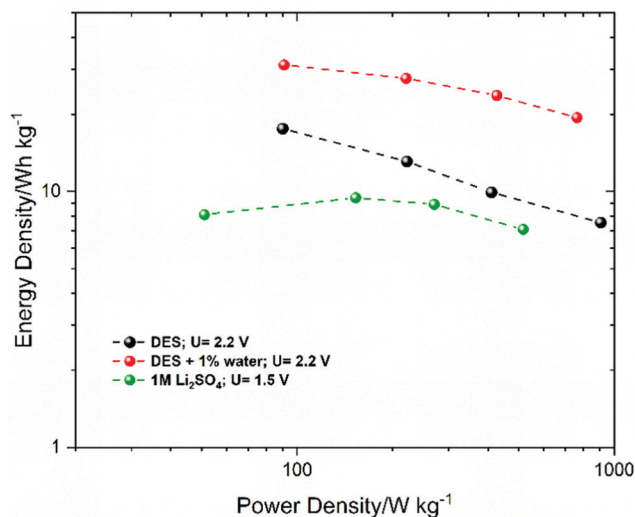


Fig. 12 Ragone plots of 3DG based supercapacitors operating in DES, DES + 1% water and $1 \text{ M Li}_2\text{SO}_4$.



Among the two DES systems, the energy density of DES + 1% water is remarkably better (19.5 W h kg^{-1}) than that of the pure DES-based system (7 W h kg^{-1}) at a 1 kW kg^{-1} power density. Compared to the Li_2SO_4 electrolyte based supercapacitor, by using the DES-based systems (DES and DES + 1% water), the Ragone plot displays an increase in the energy density of the system which highlights the importance of the Reline deep eutectic solvent. Most notably, the DES system proposed in this work has, in addition to its attractive characteristics such as being a green, low-cost and biodegradable electrolyte, beneficial features of a higher stable operating voltage window, a large specific capacity and a better energy density compared to the aqueous systems, rendering it one of the promising electrolytes for the future of electrochemical energy storage systems. The benefits of Reline-based electrolytes are summarized in Table S2 (ESI[†]). Compared to the other DES-based systems, Reline exhibits the highest cycling stability, with a wide voltage window. Construction and operation of the studied low-cost EC were performed in ambient conditions.

Conclusions

For the first time, a deep eutectic solvent based on choline chloride and urea, called Reline, has been developed as an environmentally friendly, low-cost and anti-corrosive electrolyte for supercapacitors. The thermophysical properties, high stable electrochemical window and the ability to suppress corrosion even with a 1% water content make it a promising electrolyte for electrochemical capacitors. Thanks to these properties, in this work, it was possible to use DESs as green electrolytes with a high cell voltage of up to 2.2 V.

Moreover, it has been demonstrated that, when adding water to the DES-based system, its viscosity decreases, which increases the conductivity of the electrolyte and thus ensures better performance of the electrochemical energy storage system. It has been shown after testing different percentages of water the DES + 1% water mixture displays the highest specific capacitance (157 F g^{-1}), energy density and cyclic stability. Yet, the DES + 5% water mixture presents an unstable electrochemical behavior resulting from the electrolyte decomposition. Besides the high specific capacitance, the electrochemical devices based on the 3DG electrode material and DES + 1% water show a high capacitance retention of 88% for more than 25 000 cycles at 1 A g^{-1} .

On the other hand, the cyclic stability of the pure DES electrolyte based supercapacitor using 3DG displays a supreme performance with 90% capacitance retention up to 50 000 cycles at 1 A g^{-1} which highlights the usefulness of this anti-corrosive deep eutectic solvent. Additionally, it has been proven that DES electrolytes can serve perfectly as ionic conductors for supercapacitors based on YP80F and BP2000 electrodes with an excellent electrochemical performance at a high voltage of 2.2 V.

The evidence from this study points towards the importance of the novel Reline DES as a safe, eco-friendly, low-cost and

anticorrosive supercapacitor electrolyte with competitive properties, namely, the ease of synthesis and operation in ambient conditions, availability and biodegradability, among others.

Author contributions

S. A.: conceptualization, writing – original draft, investigation, data curation, methodology, validation; M. F. K.: investigation, data curation, writing – original draft, validation; E. F.: conceptualization, supervision, resources, funding acquisition, writing – review & editing.

Conflicts of interest

There are no conflicts to declare.

Acknowledgements

The authors would like to acknowledge the OPUS project financed by the National Science Centre, Poland (project no. 2018/31/B/ST4/01852) for the financial support of the research. The Polish Ministry of Science and Higher Education is also acknowledged for the partial support (project 0911/SBAD/2101).

References

- 1 J. R. Miller and P. Simon, Electrochemical capacitors for energy management, *Science*, 2008, **321**, 651–652.
- 2 F. Pettersson, J. Keskinen, T. Remonen, L. von Hertzen, E. Jansson, K. Tappura, Y. Zhang, C.-E. Wilén and R. Österbacka, Printed environmentally friendly supercapacitors with ionic liquid electrolytes on paper, *J. Power Sources*, 2014, **271**, 298–304.
- 3 Y. Zhou, H. Qi, J. Yang, Z. Bo, F. Huang, M. S. Islam, X. Lu, L. Dai, R. Amal, C. H. Wang and Z. Han, Two-birds-one-stone: multifunctional supercapacitors beyond traditional energy storage, *Energy Environ. Sci.*, 2021, **14**, 1854–1896.
- 4 K. Fic, A. Platek, J. Piwek, J. Menzel, A. Ślesiński, P. Bujewska, P. Galek and E. Frackowiak, Revisited insights into charge storage mechanisms in electrochemical capacitors with Li_2SO_4 -based electrolyte, *Energy Storage Mater.*, 2019, **22**, 1–14.
- 5 L. H. Xu, D. Wu, M. Zhong, G. B. Wang, X. Y. Chen and Z. J. Zhang, The construction of a new deep eutectic solvents system based on choline chloride and butanediol: the influence of the hydroxyl position of butanediol on the structure of deep eutectic solvent and supercapacitor performance, *J. Power Sources*, 2021, **490**, 229365.
- 6 E. Frackowiak and F. Béguin, Carbon materials for the electrochemical storage of energy in capacitors, *Carbon*, 2001, **39**, 937–950.
- 7 H. Tabassum, A. Mahmood, B. Zhu, Z. Liang, R. Zhong, S. Guo and R. Zou, Recent advances in confining metal-based nanoparticles into carbon nanotubes for electrochemical energy



- conversion and storage devices, *Energy Environ. Sci.*, 2019, **12**, 2924–2956.
- 8 D. Zhou, H. Wang, N. Mao, Y. Chen, Y. Zhou, T. Yin, H. Xie, W. Liu, S. Chen and X. Wang, High energy supercapacitors based on interconnected porous carbon nanosheets with ionic liquid electrolyte, *Microporous Mesoporous Mater.*, 2017, **241**, 202–209.
 - 9 G. Lota, K. Fic and E. Frackowiak, Carbon nanotubes and their composites in electrochemical applications, *Energy Environ. Sci.*, 2011, **4**, 1592.
 - 10 K. Fic, M. Meller and E. Frackowiak, Strategies for enhancing the performance of carbon/carbon supercapacitors in aqueous electrolytes, *Electrochim. Acta*, 2014, **128**, 210–217.
 - 11 A. Ghosh and Y. H. Lee, Carbon-Based Electrochemical Capacitors, *ChemSusChem*, 2012, **5**, 480–499.
 - 12 X. Gao, C. Liu, G. Han, H. Song, Y. Xio and H. Zhou, Reduced graphene oxide hydrogels prepared in the presence of phenol for high-performance electrochemical capacitors, *New Carbon Mater.*, 2019, **34**, 403–416.
 - 13 P. Chen, J. Yang, S. Li, Z. Wang, T. Xiao, Y. Qian and S. Yu, Hydrothermal synthesis of macroscopic nitrogen-doped graphene hydrogels for ultrafast supercapacitor, *Nano Energy*, 2013, **2**, 249–256.
 - 14 C. Hu, L. Song, Z. Zhang, N. Chen, Z. Feng and L. Qu, Tailored graphene systems for unconventional applications in energy conversion and storage devices, *Energy Environ. Sci.*, 2015, **8**, 31–54.
 - 15 K. Fic, A. Platek, J. Piwek and E. Frackowiak, Sustainable materials for electrochemical capacitors, *Mater. Today*, 2018, **21**, 437–454.
 - 16 R. B. Leron and M.-H. Li, High-pressure density measurements for choline chloride: urea deep eutectic solvent and its aqueous mixtures at $T = (298.15 \text{ to } 323.15) \text{ K}$ and up to 50 MPa, *J. Chem. Thermodyn.*, 2012, **54**, 293–301.
 - 17 S. Sathyamoorthi, N. Phattharasupakun and M. Sawangprhruk, Environmentally benign non-fluoro deep eutectic solvent and free-standing rice husk-derived bio-carbon based high-temperature supercapacitors, *Electrochim. Acta*, 2018, **286**, 148–157.
 - 18 A. M. Navarro-Suárez and P. Johansson, Perspective—Semi-Solid Electrolytes Based on Deep Eutectic Solvents: Opportunities and Future Directions, *J. Electrochem. Soc.*, 2020, **167**, 070511.
 - 19 A. P. Abbott, G. Capper, D. L. Davies, R. K. Rasheed and V. Tambyrajah, Novel solvent properties of choline chloride/urea mixtures, *Chem. Commun.*, 2003, 70–71.
 - 20 A. P. Abbott, K. E. Ttaib, G. Frisch, K. J. McKenzie and K. S. Ryder, Electrodeposition of copper composites from deep eutectic solvents based on choline chloride, *Phys. Chem. Chem. Phys.*, 2009, **11**, 4269–4277.
 - 21 A. P. Abbott, K. E. Ttaib, G. Frisch, K. S. Ryder and D. Weston, The electrodeposition of silver composites using deep eutectic solvents, *Phys. Chem. Chem. Phys.*, 2012, **14**, 2443–2449.
 - 22 D. Fuchs, B. C. Bayer, T. Gupta, G. L. Szabo, R. A. Wilhelm, D. Eder, J. C. Meyer, S. Steiner and B. Gollas, Electrochemical Behavior of Graphene in a Deep Eutectic Solvent, *ACS Appl. Mater. Interfaces*, 2020, **12**, 40937–40948.
 - 23 L. I. N. Tomé, V. Baião, W. da Silva and C. M. A. Brett, Deep eutectic solvents for the production and application of new materials, *Appl. Mater. Today*, 2018, **10**, 30–50.
 - 24 S. T. Williamson, K. Shahbaz, F. S. Mjalli, I. M. Al Nashef and M. M. Farid, Application of deep eutectic solvents as catalysts for the esterification of oleic acid with glycerol, *Renew. Energy*, 2017, **114**, 480–488.
 - 25 I. Juneidi, M. Hayyan and M. A. Hashim, Intensification of biotransformations using deep eutectic solvents: Overview and outlook, *Process Biochem.*, 2018, **66**, 33–60.
 - 26 J. Huang, X. Guo, T. Xu, L. Fan, X. Zhou and S. Wu, Ionic deep eutectic solvents for the extraction and separation of natural products, *J. Chromatogr. A*, 2019, **1598**, 1–19.
 - 27 K. Zhang, Y. Hou, Y. Wang, K. Wang, S. Ren and W. Wu, Efficient and Reversible Absorption of CO₂ by Functional Deep Eutectic Solvents, *Energy Fuels*, 2018, **32**, 7727–7733.
 - 28 J. Patiño, M. C. Gutiérrez, D. Carriazo, C. O. Ania, J. B. Parra, M. L. Ferrer and F. del Monte, Deep eutectic assisted synthesis of carbon adsorbents highly suitable for low-pressure separation of CO₂-CH₄ gas mixtures, *Energy Environ. Sci.*, 2012, **5**, 8699–8707.
 - 29 V. S. Protsenko, T. E. Butyrina, L. S. Bobrova, S. A. Korniy and F. I. Danilov, Enhancing corrosion resistance of nickel surface by electropolishing in a deep eutectic solvent, *Mater. Lett.*, 2020, **270**, 127719.
 - 30 A. P. Abbott, D. Boothby, G. Capper, D. L. Davies and R. K. Rasheed, Deep Eutectic Solvents Formed between Choline Chloride and Carboxylic Acids: Versatile Alternatives to Ionic Liquids, *J. Am. Chem. Soc.*, 2004, **126**, 9142–9147.
 - 31 S. Wang, Z. Zhang, Z. Lu and Z. Xu, A novel method for screening deep eutectic solvent to recycle the cathode of Li-ion batteries, *Green Chem.*, 2020, **22**, 4473–4482.
 - 32 B. Chakrabarti, J. Rubio-García, E. Kalamaras, V. Yufit, F. Tariq, C. T. J. Low, A. Kucernak and N. Brandon, Evaluation of a Non-Aqueous Vanadium Redox Flow Battery Using a Deep Eutectic Solvent and Graphene-Modified Carbon Electrodes via Electrophoretic Deposition, *Batteries*, 2020, **6**, 38.
 - 33 Y. Wang and H. Zhou, A green and cost-effective rechargeable battery with high energy density based on a deep eutectic catholyte, *Energy Environ. Sci.*, 2016, **9**, 2267–2272.
 - 34 M. B. Karimi, F. Mohammadi and K. Hooshyari, Non-humidified fuel cells using a deep eutectic solvent (DES) as the electrolyte within a polymer electrolyte membrane (PEM): the effect of water and counterions, *Phys. Chem. Chem. Phys.*, 2020, **22**, 2917–2929.
 - 35 H.-R. Jhong, D. S.-H. Wong, C.-C. Wan, Y.-Y. Wang and T.-C. Wei, A novel deep eutectic solvent-based ionic liquid used as electrolyte for dye-sensitized solar cells, *Electrochem. Commun.*, 2009, **11**, 209–211.
 - 36 G. Li, H. Yang, D. Zuo, J. Xu and H. Zhang, Deep eutectic solvent-based supramolecular gel polymer electrolytes for high-performance electrochemical double layer capacitors, *Int. J. Hydrogen Energy*, 2021, S0360319921003086.



- 37 V. K. Vorobiov, M. A. Smirnov, N. V. Bobrova and M. P. Sokolova, Chitosan-supported deep eutectic solvent as bio-based electrolyte for flexible supercapacitor, *Mater. Lett.*, 2021, **283**, 128889.
- 38 M. Zhong, Q. F. Tang, Y. W. Zhu, X. Y. Chen and Z. J. Zhang, An alternative electrolyte of deep eutectic solvent by choline chloride and ethylene glycol for wide temperature range supercapacitors, *J. Power Sources*, 2020, **452**, 227847.
- 39 W. Zaidi, A. Boisset, J. Jacquemin, L. Timperman and M. Anouti, Deep Eutectic Solvents Based on N-Methylacetamide and a Lithium Salt as Electrolytes at Elevated Temperature for Activated Carbon-Based Supercapacitors, *J. Phys. Chem. C*, 2014, **118**, 4033–4042.
- 40 D. Wu, L. H. Xu, H. J. Feng, Y. W. Zhu, X. Y. Chen and P. Cui, Design and theoretical study of novel deep eutectic solvents: The effects of bromine and chloride anions on solvation structure and supercapacitor performance, *J. Power Sources*, 2021, **492**, 229634.
- 41 S. Amara, W. Zaidi, L. Timperman, G. Nikiforidis and M. Anouti, Amide-based deep eutectic solvents containing LiFSI and NaFSI salts as superionic electrolytes for supercapacitor applications, *J. Chem. Phys.*, 2021, **154**, 164708.
- 42 S. S. Karade, S. Lalwani, J.-H. Eum and H. Kim, Sustain. Deep eutectic solvent-assisted synthesis of RuCo₂O₄: an efficient positive electrode for hybrid supercapacitors, *Energy Fuels*, 2020, **4**, 3066–3076.
- 43 P. Kumari, Shobhna, S. Kaur and H. K. Kashyap, Influence of Hydration on the Structure of Reline Deep Eutectic Solvent: A Molecular Dynamics Study, *ACS Omega*, 2018, **3**, 15246–15255.
- 44 S. H. Zeisel and K.-A. da Costa, Choline: an essential nutrient for public health, *Nutr. Rev.*, 2009, **67**, 615–623.
- 45 S. Björklund, J. Engblom, K. Thuresson and E. Sparr, Glycerol and urea can be used to increase skin permeability in reduced hydration conditions, *Eur. J. Pharm. Sci.*, 2013, **50**, 638–645.
- 46 J. G. Driver, R. E. Owen, T. Makanyire, J. A. Lake, J. McGregor and P. Styring, Blue Urea: Fertilizer With Reduced Environmental Impact, *Front. Energy Res.*, 2019, **7**, 28.
- 47 H. J. S. Finch, A. M. Samuel and G. P. F. Lane, 4 – Fertilisers and manures, in *Lockhart & Wiseman's Crop Husbandry Including Grassland*, Ninth Edition, ed. H. J. S. Finch, A. M. Samuel and G. P. F. Lane, Woodhead Publishing, 2014, pp. 63–91.
- 48 U. Mahanta, S. Choudhury, R. P. Venkatesh, S. Sarojiniamma, S. A. Ilangovan and T. Banerjee, Ionic-Liquid-Based Deep Eutectic Solvents as Novel Electrolytes for Supercapacitors: COSMO-SAC Predictions, Synthesis, and Characterization, *ACS Sustainable Chem. Eng.*, 2020, **8**, 372–381.
- 49 T. Hassan Ibrahim, R. Alhasan, M. Bedrelzaman, M. Sabri, N. Jabbar and F. Mjalli, Corrosion Behavior of Common Metals in Eutectic Ionic Liquids, *Int. J. Electrochem. Sci.*, 2019, **14**, 8450–8469.
- 50 A. P. Abbott, E. I. Ahmed, R. C. Harris and K. S. Ryder, Evaluating water miscible deep eutectic solvents (DESs) and ionic liquids as potential lubricants, *Green Chem.*, 2014, **16**, 4156–4161.
- 51 A. Yadav and S. Pandey, Densities and Viscosities of (Choline Chloride + Urea) Deep Eutectic Solvent and Its Aqueous Mixtures in the Temperature Range 293.15 K to 363.15 K, *J. Chem. Eng. Data*, 2014, **59**, 2221–2229.
- 52 C. Du, B. Zhao, X.-B. Chen, N. Birbilis and H. Yang, Effect of water presence on choline chloride-2urea ionic liquid and coating platings from the hydrated ionic liquid, *Sci. Rep.*, 2016, **6**, 29225.
- 53 D. Lapeña, F. Bergua, L. Lomba, B. Giner and C. Lafuente, A comprehensive study of the thermophysical properties of reline and hydrated reline, *J. Mol. Liq.*, 2020, **303**, 112679.
- 54 L. Sapir and D. Harries, Restructuring a Deep Eutectic Solvent by Water: The Nanostructure of Hydrated Choline Chloride/Urea, *J. Chem. Theory Comput.*, 2020, **16**, 3335–3342.
- 55 A. Y. M. Al-Murshedi, H. F. Alesary and R. Al-Hadrawi, Thermophysical properties in deep eutectic solvents with/without water, *J. Phys. Conf. Ser.*, 2019, **1294**, 052041.
- 56 T. Zhekenov, N. Toksanbayev, Z. Kazakbayeva, D. Shah and F. S. Mjalli, Formation of type III Deep Eutectic Solvents and effect of water on their intermolecular interactions, *Fluid Phase Equilib.*, 2017, **441**, 43–48.
- 57 S. Pal and S. Paul, Understanding The Role of Reline, a Natural DES, on Temperature-Induced Conformational Changes of C-Kit G-Quadruplex DNA: A Molecular Dynamics Study, *J. Phys. Chem. B*, 2020, **124**, 3123–3136.
- 58 S. Kaur, S. Sharma and H. K. Kashyap, Bulk and interfacial structures of reline deep eutectic solvent: a molecular dynamics study, *J. Chem. Phys.*, 2017, **147**, 194507.
- 59 M. Foroutan and L. Naji, Systematic evaluation of factors influencing electrochemical and morphological characteristics of free-standing 3D graphene hydrogels as electrode material for supercapacitors, *Electrochim. Acta*, 2019, **301**, 421–435.
- 60 Q. Zhang, K. De Oliveira Vigier, S. Royer and F. Jérôme, Deep eutectic solvents: syntheses, properties and applications, *Chem. Soc. Rev.*, 2012, **41**, 7108.
- 61 S. G. Rathod, R. F. Bhajantri, V. Ravindrachary, P. K. Pujari, G. K. Nagaraja, J. Naik, V. Hebbar and H. Chandrappa, Temperature-dependent ionic conductivity and transport properties of LiClO₄-doped PVA/modified cellulose composites, *Bull. Mater. Sci.*, 2015, **38**, 1213–1221.
- 62 J. Jacquemin, P. Husson, A. A. H. Padua and V. Majer, Density and viscosity of several pure and water-saturated ionic liquids, *Green Chem.*, 2006, **8**, 172–180.
- 63 Y. Wang, W. Chen, Q. Zhao, G. Jin, Z. Xue, Y. Wang and T. Mu, Ionicity of deep eutectic solvents by Walden plot and pulsed field gradient nuclear magnetic resonance (PFG-NMR), *Phys. Chem. Chem. Phys.*, 2020, **22**, 25760–25768.
- 64 D. Farhat, D. Lemordant, J. Jacquemin and F. Ghamouss, Alternative Electrolytes for Li-Ion Batteries Using Glutaronitrile and 2-methylglutaronitrile with Lithium Bis(trifluoromethanesulfonyl) Imide, *J. Electrochem. Soc.*, 2019, **166**, A3487–A3495.
- 65 A. Boisset, J. Jacquemin and M. Anouti, Physical properties of a new Deep Eutectic Solvent based on lithium



- bis[(trifluoromethyl)sulfonyl]imide and *N*-methylacetamide as superionic suitable electrolyte for lithium ion batteries and electric double layer capacitors, *Electrochim. Acta*, 2013, **102**, 120–126.
- 66 U. A. Rana, R. Vijayaraghavan, M. Walther, J. Sun, A. A. J. Torriero, M. Forsyth and D. R. MacFarlane, Protic ionic liquids based on phosphonium cations: comparison with ammonium analogues, *Chem. Commun.*, 2011, **47**, 11612.
- 67 M. H. Mamme, S. L. C. Moors, H. Terryn, J. Deconinck, J. Ustarroz and F. De, Proft, Atomistic Insight into the Electrochemical Double Layer of Choline Chloride–Urea Deep Eutectic Solvents: Clustered Interfacial Structuring, *J. Phys. Chem. Lett.*, 2018, **9**, 6296–6304.
- 68 K. Xu, S. P. Ding and T. R. Jow, Toward Reliable Values of Electrochemical Stability Limits for Electrolytes, *J. Electrochem. Soc.*, 1999, **146**, 4172–4178.
- 69 X. Ge, C. Gu, X. Wang and J. Tu, Deep eutectic solvents (DESS)-derived advanced functional materials for energy and environmental applications: challenges, opportunities, and future vision, *J. Mater. Chem. A*, 2017, **5**, 8209–8229.

